UNIVERSAL MULTIPLICITY AND p_T-distributions AND PERCOLATION OF STRINGS

ISMD KRAKÓW Sept 2003

C. Pajares Univ Santiago de COMPOSTELA

- INTRODUCTION
- MULTIPLICITIES. N_{part} scaling
- CLUSTER SIZE DISTRIBUTIONS
- p_T distributions
- n distributions
- CONCLUSIONS

J. Dias de Deus (IST LISBON) R. Ugoccioni (Torino)
M. A. Braun (Univ St Petersbourg)
E. G. Ferreiro, F. del Moral (Santiago)

High energy nucleus collisions → Interaction between two clouds of partons

Each parton-parton interaction → string located in impact parameter space

As engy and size of projectile and target increases, the density of strings increases

The behaviour of the percolating system is governed by the parameter

density of strings

$$\eta = \pi r_0^2 n = \frac{\pi r_0^2}{S} N$$

NUMBER of EXCHANGED STRINGS

πr_0^2 → transverse size of one string

S → total available transverse area

Percolation occurs when a path of overlapping strings is formed through the total nuclear transverse area. This happens above a <u>critical density of strings</u>

For $r_0 \simeq 0.2 \text{ fm} - 0.25 \text{ fm}$ $\eta_c = 1.18 - 1.5$

i.e. 7-9 strings / fm^2

The fraction of surface occupied by strings is

$$\phi = 1 - e^{-\eta}$$

$$\vec{Q}_n^{\,2} = (\vec{Q}_1 + \cdots + \vec{Q}_1)^2$$

$$\langle \vec{Q}_i \vec{Q}_j \rangle = 0$$

$$Q_n^2 = n Q_1^2$$

$$\mu_n = \sqrt{\frac{n S_n}{S_1}}\, \mu_1$$

just touching 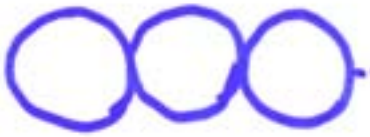 $S_n = n S_1$

$\mu_n = n \mu_1$ No supression

Maximum overlapping

 $S_n = S_1$ $\mu_n = \sqrt{n}\, \mu_1$

(Max supression)

$$\mu_n = \sqrt{\frac{n S_n}{S_1}}\,\mu_1$$

$$\langle p_T^2 \rangle_n = \sqrt{\frac{n S_n}{S_n}}\,\langle p_T^2 \rangle_1$$

(Schwinger formula)

In the thermodynamical limit

$$\left\langle n \frac{S_1}{S_n} \right\rangle \longrightarrow \frac{1}{F^2(\eta)} \qquad F(\eta) = \sqrt{\frac{1-e^{-\eta}}{\eta}}$$

Notice

$$\mu_n \langle p_T^2 \rangle_n = n\, \mu_1 \langle p_T^2 \rangle_1$$

and

$$\frac{\mu_n}{\langle p_T^2 \rangle_n} = \frac{S_n}{S_1}\,\frac{\mu_1}{\langle p_T^2 \rangle_1} \longrightarrow \frac{\pi R^2}{\pi r_0^2}\,\frac{\mu_1}{\langle p_T^2 \rangle_1}$$

$$\boxed{\frac{\mu}{\langle p_T^2 \rangle} \approx \frac{\pi R^2}{\pi r_0^2}\,\frac{\mu_1}{\langle p_T^2 \rangle_1}}$$

We generate the strings following the DPM or QGSM using a Monte-Carlo code. Each string is located in impact parameter plane and therefore we identify the formed clusters for each event and their corresponding cluster surface. For each cluster we compute $\langle \mu_n \rangle$ and $\langle p_T^2 \rangle_n$

$$\left.\frac{dN_{ch}}{d\eta d^2p_T}\right|_{\eta=0} \propto g(s) N_{strings} F(\eta) \underset{\text{high density}}{\propto} N_A^{4/3} \frac{1}{\sqrt{\eta}} =$$

$$= N_A^{4/3} \frac{1}{\sqrt{\frac{N_A^{4/3}}{N_A^{2/3}} s_0^2}} = N_A$$

$$\left.\frac{\frac{dN_{ch}}{d\eta d^2p_T}}{N_A}\right|_{\eta=0} \propto g(p_T)$$

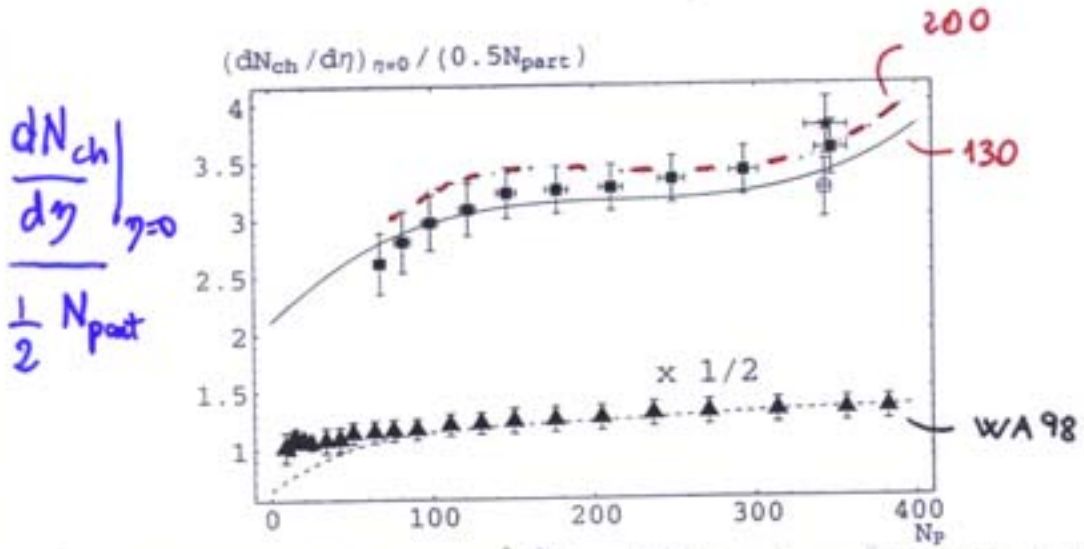

FIG. 1. Comparison of the dependence of the multiplicity on the number of participants with the SPS WA98 [16] data (filled triangles), with the RHIC PHENIX [5] (filled boxes) and PHOBOS [6] (non-filled boxes) data at $\sqrt{s} = 130$ GeV and with PHIC PHENIX data at $\sqrt{200}$ GeV (filled stars) . The dashed, solid and dotted lines are our predictions for the relevant energies.

M. Braun, F. del Moral & C P PRC 65, 024907 Percolation (2002)

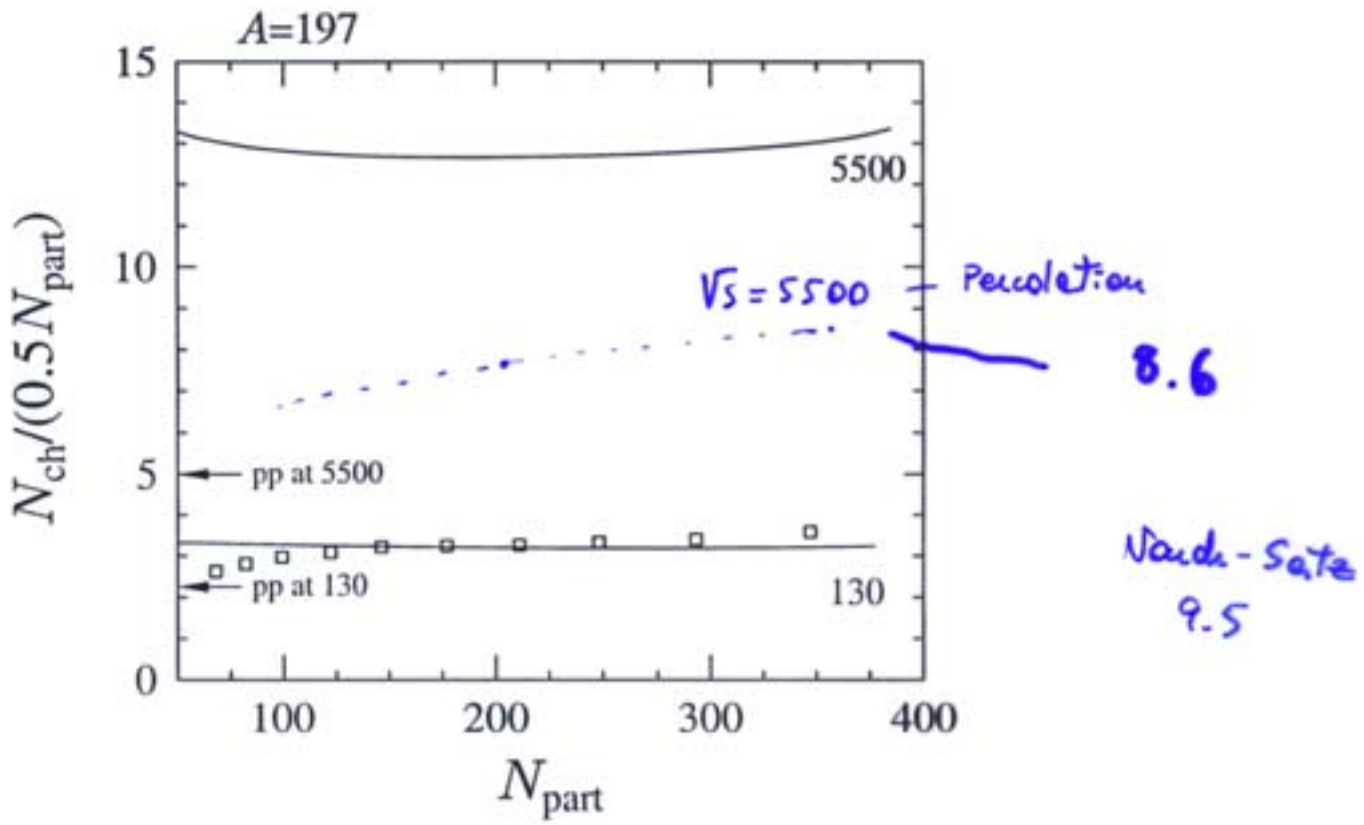

Figure 4: Rapidity density of charged particles near $y = 0$ per 0.5 times the number of participants at LHC and RHIC energies computed using the local saturation criterion in [8]. RHIC data at $\sqrt{s} = 130$ GeV [2] (open squares) and p+p rapidity densities (then $N_{\rm part} = 2$; arrows) are also shown. Large (small) $N_{\rm part}$ corresponds to central $\mathbf{b} = 0$ (peripheral, $\mathbf{b} \to 2R_A$) collisions.

Eskola et al

Higher centrality → changes in the cluster size probability

trigger on higher centrality means transformations of type

$$P(m) \longrightarrow \frac{m\,P(m)}{\langle m \rangle} \longrightarrow \cdots \frac{m^k}{\langle m^k \rangle} P(m)$$

6. Jona Lasinio (The renormalization group : A probabilistic view Nuovo Cim 26B 99 (1975)

J. Dias de Deus, C. P., C. A. Salgado PLB 408 417 (97) PLB 409 474 (1997)

resulting

$$P(m) \sim m^k \exp(-\gamma m)$$

k increases with centrality

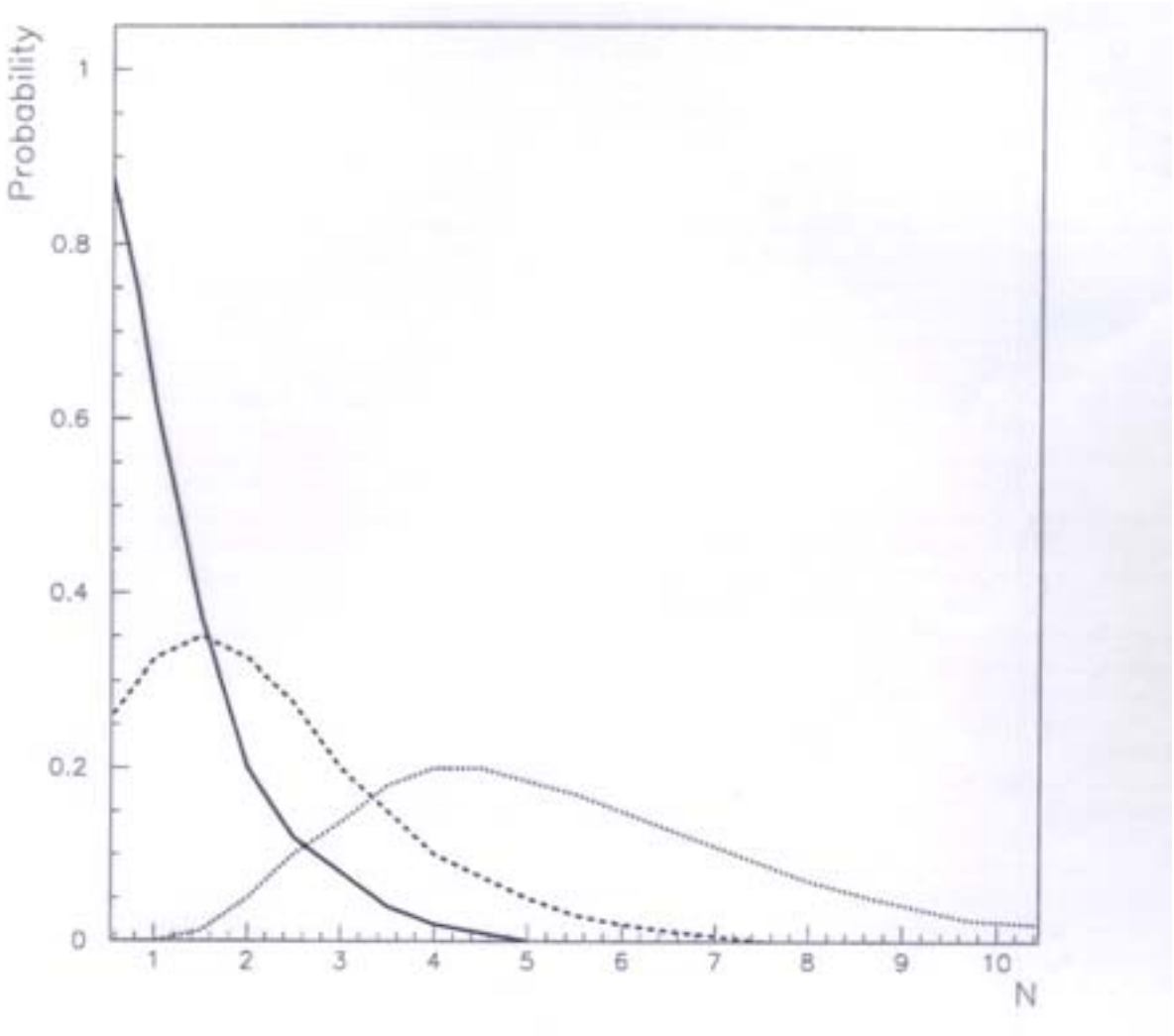

FIG. 1. Schematic representation of the number of clusters as a function of the number of strings of each cluster at three different centralities (the continuous line corresponds to the most peripherical one and the pointed line to the most central one)

If $1/K$ is the width of the distribution,

K large at very low density (γ)
(only clusters of 1 string)

K decreases with γ at low γ

K increases with γ at higher γ
(only clusters with many strings)

Let assume a distribution of the type

$$\frac{\gamma}{\Gamma(K)} (\gamma x)^{K-1} \exp(-\gamma x)$$

p_T distributions

Assumption : clusters decay $\exp(-p_T^2 x)$

x depends on the number of strings of the cluster

$$\left(1 + \frac{p_T^2}{\lambda_0 k}\right)^{-k} = \int_0^\infty dx\, e^{-p_T^2 x} \underbrace{\frac{\gamma}{\Gamma(k)} (\gamma x)^{k-1} e^{-\gamma x}}_{P(x)}$$

$\lambda_0 k = \gamma$

i) $\langle x \rangle = \frac{k}{\gamma}$

ii) $\frac{\langle x^2 \rangle - \langle x \rangle^2}{\langle x \rangle^2} = \frac{1}{k}$

iii) $\langle x \rangle P(x) = \frac{k}{\Gamma(k)} \left(\frac{kx}{\langle x \rangle}\right)^{k-1} e^{-\frac{kx}{\langle x \rangle}} = f\left(\frac{x}{\langle x \rangle}\right)$

If k does not depend on energy is KNO

iv) $\begin{cases} x \to \lambda x \\ \gamma \to \gamma/\lambda \end{cases}$ This invariance, implies a change $p_T^2 \to p_T^2 \lambda$ in the total distribution

v) At $\gamma \to \infty$, $k \to \infty$ $P(x) \to \delta(x - x_0)$, $e^{-p_T^2/\lambda_0}$

$$\langle p_T^2\rangle_1 \longrightarrow \langle p_T^2\rangle_m = \sqrt{\frac{m S_1}{S_m}}\,\langle p_T^2\rangle_1 \approx \frac{1}{F(\eta)}\,\langle p_T^2\rangle_1$$

$$\langle n\rangle_1 \longrightarrow \langle n\rangle_m = \sqrt{\frac{m S_m}{S_1}}\,\langle n\rangle_1 \approx m\,F(\eta)\,\langle n\rangle_1$$

$$F(\eta) = \sqrt{\frac{1-e^{-\eta}}{\eta}}$$

$$\eta = \frac{N_s S_1}{S_{AA}}$$

Then the total

$\langle p_T^2\rangle \neq \langle p_T^2\rangle_1$ and $\langle n\rangle \neq N_s \langle n\rangle_1$

but

$$\begin{cases} \langle p_T^2\rangle = \dfrac{1}{F(\eta)}\langle p_T^2\rangle_1 = \dfrac{1}{F(\eta)}\langle p_T^2\rangle_{old} \\ \langle n\rangle = N_s F(\eta)\langle n\rangle_1 = F(\eta)\langle n\rangle_{old} \end{cases}$$

This means $\lambda = F(\eta)$ and

the p_T distribution is

$$\left(1 + \frac{F(\eta)\,p_T^2}{\lambda_0 K = \gamma}\right)^{-K}$$

or $p_T^2 \longrightarrow m_T^2$

Assuming that the clusters give rise to Poisson multiplicities

$$\int_0^\infty dy\, e^{-y}\frac{y^n}{n!}\underbrace{\frac{\gamma}{\Gamma(k)}(\gamma y)^{k-1}\exp(-\gamma y)}_{P(y)} =$$

$$= \frac{\Gamma(k+n)}{\Gamma(1+n)\Gamma(k)}\frac{\gamma^k}{(1+\gamma)^{k+n}} \qquad \text{(NBD)}$$

$$P(n) = \int d\mu\, \underbrace{P(n,\mu)}_{\text{Poisson}}\underbrace{P(\mu)}_{\text{string size distribut}}$$

$$\begin{cases} \langle n\rangle = \dfrac{k}{\gamma} = \langle y\rangle \\ \dfrac{\langle n^2\rangle - \langle n\rangle^2}{\langle n\rangle^2} = \dfrac{1}{k} + \dfrac{1}{\langle n\rangle} \end{cases}$$

$$\begin{cases} y \to \lambda' y \\ \gamma \to \gamma/\lambda' \end{cases}$$ the distribution changes $\gamma \to \gamma/\lambda'$

now $\lambda' = F(n)$

$$\frac{A}{(\gamma + F(\eta) m_T^2)^K}$$

a) K should increase with centrality for η not very small, $K \sim \frac{1}{F(\eta)}$

b) K also measures the hardness

K should decrease with energy

e^+e^-

$$P(n) \sim n^{K\mu - 1} \exp\left(-D \frac{n}{\langle n \rangle}\right)^{\mu}$$

$$\mu \sim \frac{1}{1 - \sqrt{\frac{6}{\pi}\alpha_s}}$$

c) K when $\eta \to 0$ should increase

$$K = \mu \left[\frac{3}{2} + \frac{c_1}{F(\eta)}\right] \quad c_1 = 1$$

for $\eta \geq 0.2$-

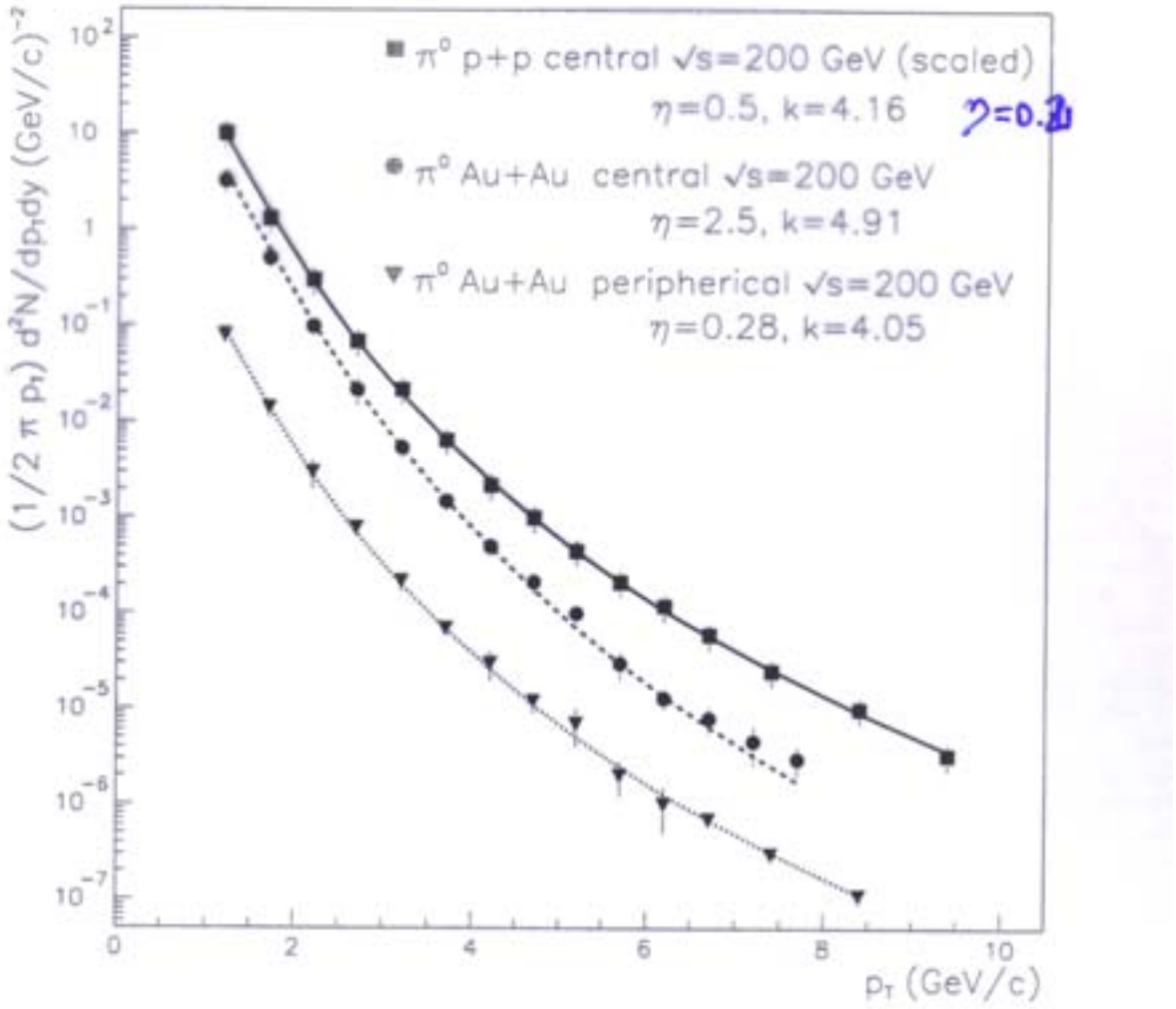

FIG. 2. Comparison between our results and experimental data from Au-Au central and peripherical collisions and p-p central collisions at $\sqrt{s} = 200$ GeV. Data are from Ref. [31].

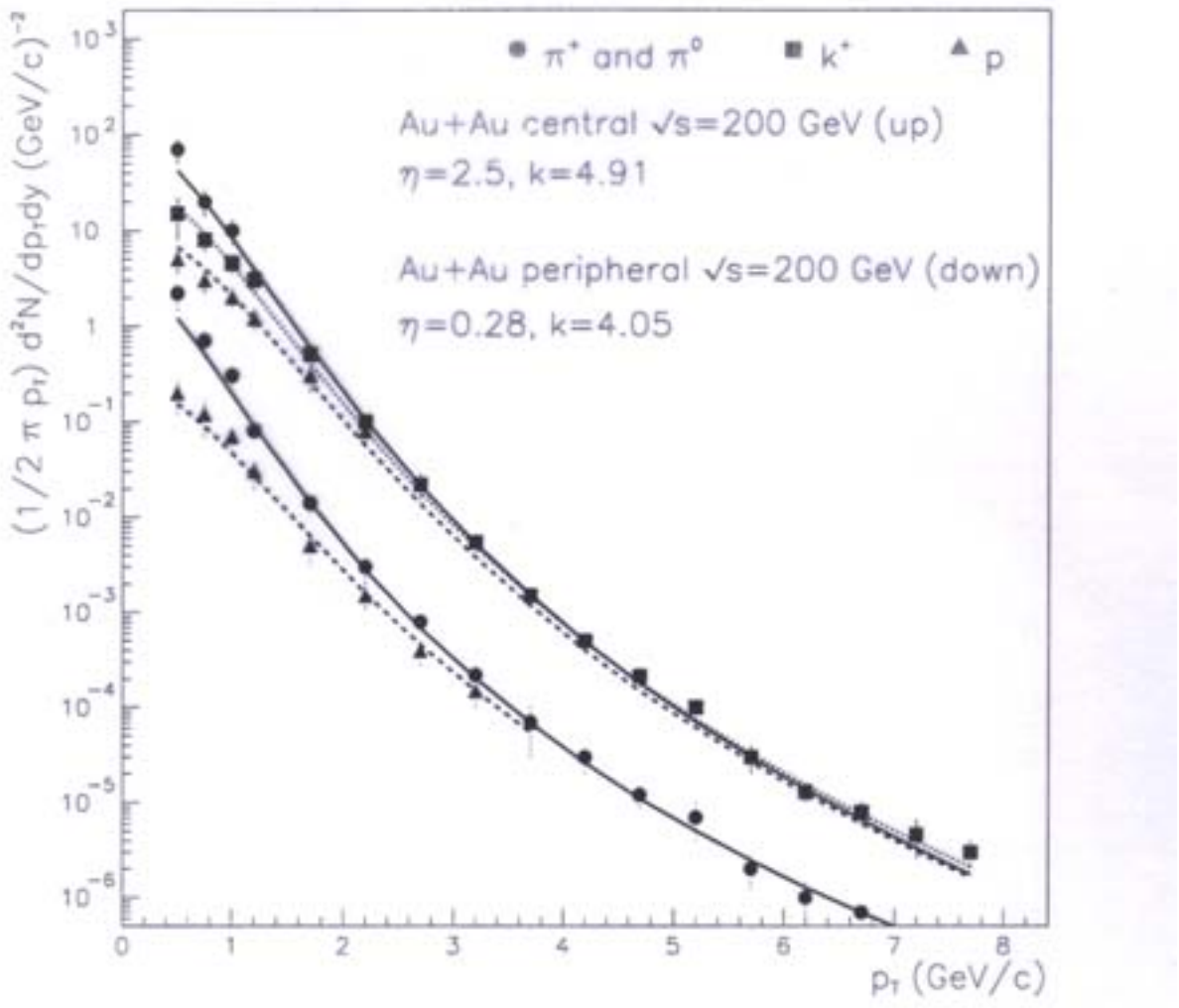

FIG. 3. Comparison between our results and experimental data from Au-Au central and peripherical collisions at $\sqrt{s} = 200$ GeV. Data are from Ref. [32].

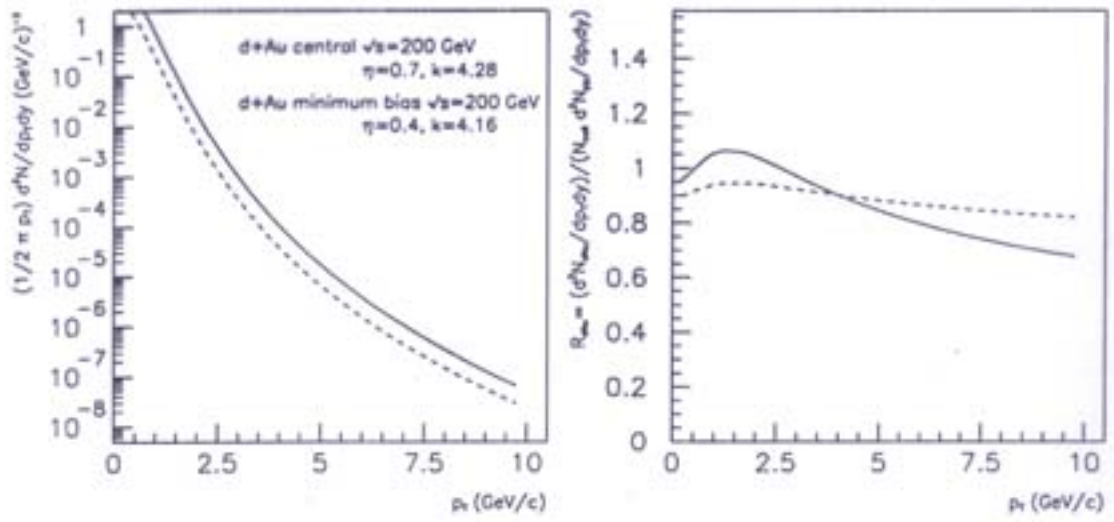

Figure 10: Our prediction for d+Au collisions at 200 GeV and different centralities

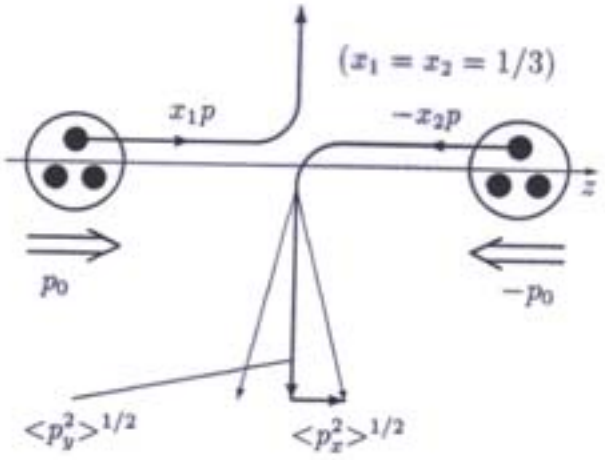

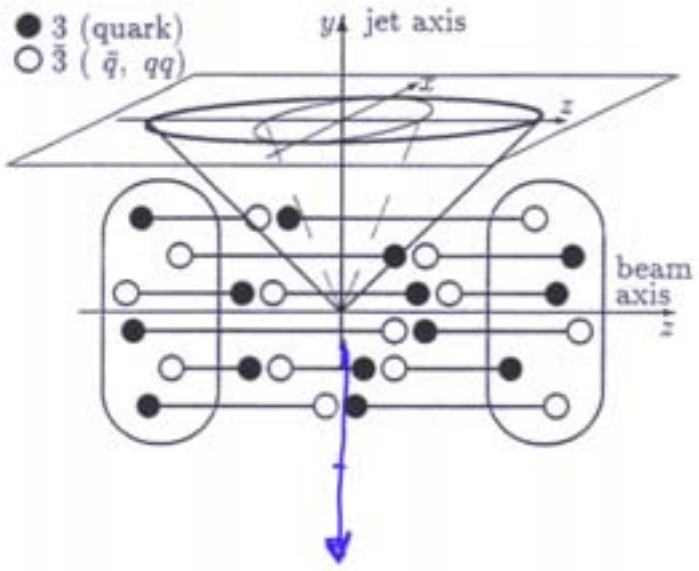

Au-Au central

$\sqrt{s} = 200$ $\quad \Delta p_z \approx 10$ GeV/c

d-Au central $\quad \Delta p_z \approx 2$ GeV/c

CONCLUSIONS

. The clustering of strings produces a supression of high p_T distributions

. The p_T distributions are related to multiplicity distributions. Supression of the tail of multiplicity distributions at high η.

. pp at higher η (LHC) will have narrower multiplicity distribution.

. The interaction of the quark jet with the strong color field makes much broader this jet in Au-Au central collisions

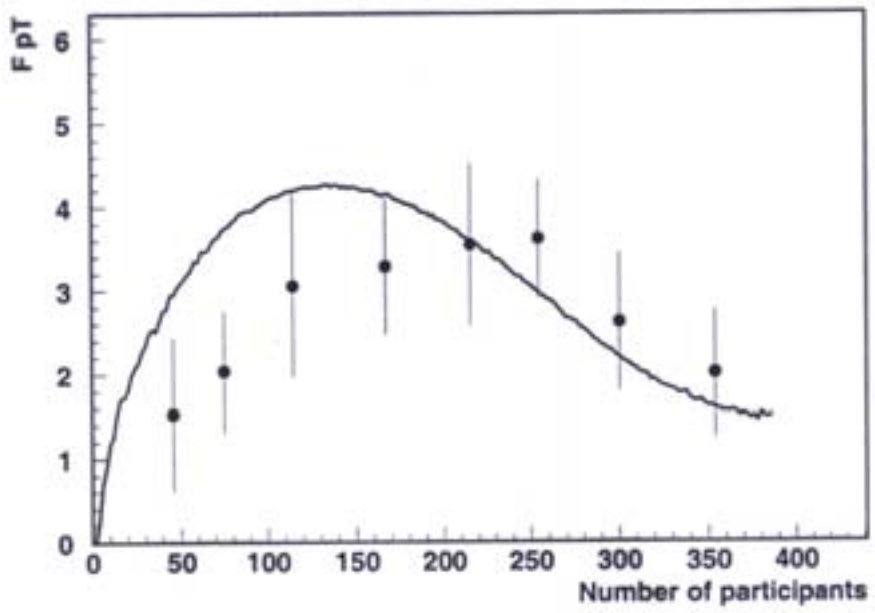

FIG. 1. F_{pT} as a function of the number of participants. Experimental data from Phenix at $\sqrt{s} = 200$ GeV are compared with our results (continuous line).